Two-Scale Stochastic Optimization for Controlling Distributed Storage Devices

Harsha Gangammanavar and Suvrajeet Sen

***Abstract*— This paper is motivated by a power system with storage devices at multiple locations which need to be controlled at a much finer timescale than that necessary for conventional generation units. We present a stochastic optimization model of the power system which captures interactions of decisions at these two timescales through a novel state-variable formulation. The model also includes transmission constraints approximated by a linearized dc network, fast response operating reserves, and renewable generation. To tackle this high-dimensional multistage stochastic optimization problem, we present a sequential sampling method which we refer to as the stochastic dynamic linear programming. This algorithm is a dynamic extension of regularized two-stage stochastic decomposition for stagewise independent multistage stochastic linear programs, and is targeted at the class of problems where decisions are made at two different timescales. We compare our algorithm with the stochastic dual dynamic programming (SDDP) which has been effectively applied in planning power systems operations. Our computational results show that our sequential Monte-Carlo approach provides prescriptive solutions and values which are statistically indistinguishable from those obtained from SDDP, while improving computational times significantly.**

***Index Terms*—Multistage stochastic programming, sampling-based algorithm, distributed storage control.**

NOMENCLATURE

Sets

$\mathcal{T}$	$:= 1, \ldots, T$, adaptive decision epochs
$\mathcal{B}$	Buses
$\mathcal{L}$	Transmission lines
$\mathcal{I}$	Intertie nodes
$\mathcal{G}$	Conventional generators
$\mathcal{W}$	Renewable generators
$\mathcal{R}$	Operating reserves
$\mathcal{N}$	Storage devices
$\mathcal{D}$	Loads. Subset $\mathcal{G}_i \subseteq \mathcal{G}$ denotes conventional generators connected to bus $i \in \mathcal{B}$. Similarly we have the subsets $\mathcal{W}_i$, $\mathcal{D}_i$, $\mathcal{N}_i$ and $\mathcal{R}_i$.

State Variables

For all $t \in \mathcal{T}$

W_{it}	Renewable generation at location $i \in \mathcal{W}$
$\tilde{\omega}_t$	$:= (\widetilde{W}_{ti})_{i\in\mathcal{W}}$, exogenous state variable
x_{it}^{store}	State of storage device $i \in \mathcal{N}$
x_{it}^{res}	State of operating reserve $i \in \mathcal{R}$
$\tilde{x}_t$	$:= ((\tilde{x}_{it}^{store})_{i\in\mathcal{N}}, (\tilde{x}_{it}^{res})_{i\in\mathcal{R}})$, endogenous state variable
$\tilde{s}_t$	$:= (u_0, \tilde{x}_t, \tilde{\omega}_t)$, system state variable. A realization of the random variable $\tilde{\omega}_t$ is denoted as ω_t. Similar notation is followed for $\tilde{x}_t$ and $\tilde{s}_t$.

Coarse Timescale Decision Variable

G_i	Conventional generation level for $i \in \mathcal{G}$
u_0	$:= (G_i)_{i\in\mathcal{G}}$, a vector of generation levels.

Fine Timescale Decision Variables

For all $t \in \mathcal{T}$

p_{ijt}	Power flow on line $(i, j) \in \mathcal{L}$
θ_{it}	Phase angle at bus $i \in \mathcal{B}$
q_{it}^+, q_{it}^-	Energy bought and sold at intertie nodes $i \in \mathcal{I}$
r_{it}	Operating reserve energy utilized at $i \in \mathcal{R}$
v_{it}^+, v_{it}^-	Storage charging and discharging for $i \in \mathcal{N}$
u_t	$:= ((p_{ijt}), (\theta_{it}), (v_{it}^+, v_{it}^-), (q_{it}^+, q_{it}^-), (r_{it}))$.
$h_0(x_0)$	Coarse timescale objective function value
$h_t(s_t)$	Recourse function/fine timescale stagewise objective function value $t \in \mathcal{T}$.

Parameters

G_i^{init}	Initial generation level for $i \in \mathcal{G}$
G_i^{min}, G_i^{max}	Generation capacity for $i \in \mathcal{G}$
$\Delta G_i^{up}, \Delta G_i^{down}$	Maximum up and down ramp capability for generator $i \in \mathcal{G}$
Λ_i	Voltage at bus $i \in \mathcal{B}$
$\theta_i^{min}, \theta_i^{max}$	Limits on phase angle at bus $i \in \mathcal{B}$
X_{ij}	Reactance of line $(i, j) \in \mathcal{L}$
$p_{ij}^{min}, p_{ij}^{max}$	Capacity of line $(i, j) \in \mathcal{L}$
V_i^{max}	Capacity of storage device $i \in \mathcal{N}$
$\Delta V_i^+, \Delta V_i^-$	Power rating (charging and discharging) of device $i \in \mathcal{N}$

Manuscript received March 10, 2016; revised June 24, 2016 and August 25, 2016; accepted October 2, 2016. Date of publication October 12, 2016; date of current version June 19, 2018. This work was supported by AFOSR under Grant FA9550-15-1-0267. The work of S. Sen was supported by NSF under Grant ECCS1548847. Paper no. TSG-00311-2016.

H. Gangammanavar is with the Department of Engineering Management, Information, and Systems, Southern Methodist University, Dallas, TX 75275 USA (e-mail: harsha@smu.edu).

S. Sen is with the Daniel J. Epstein Department of Industrial and Systems Engineering, University of Southern California, Los Angeles, CA 90089 USA (e-mail: s.sen@usc.edu).

Color versions of one or more of the figures in this paper are available online at http://ieeexplore.ieee.org.

Digital Object Identifier 10.1109/TSG.2016.2616881

ρ_i^+, ρ_i^-	Charging and discharging efficiency of device $i \in \mathcal{N}$
η_i	Storage dissipation loss factor of device $i \in \mathcal{N}$
R_i^{min}, R_i^{max}	Capacity of operating reserve $i \in \mathcal{R}$
$\Delta R_i^{down}, \Delta R_i^{max}$	Maximum up and down ramp capability of reserve $i \in \mathcal{R}$
d_i^{gen}	Unit production cost of generator $i \in \mathcal{G}$
d_i^{res}	Unit production cost of reserve $i \in \mathcal{R}$
d_i^{buy}, d_i^{sell}	Unit transaction (buy/sell) cost at bus $i \in \mathcal{I}$
c_i^{store}	Unit storage cost at $i \in \mathcal{N}$
D_{it}	Demand at $i \in \mathcal{D}$ in time period $t \in \mathcal{T}$.

I. Introduction

A KEY focus of modernizing the electricity grid is reducing the dependence on fossil fuels and relying on large scale integration of renewable resources. This is driven by the rising concerns due to climate change, state incentives including renewable portfolio standards, and consumer efforts. Unlike dispatchable energy resources, which meet the majority of the current electricity demand, renewable resources have variable and intermittent output. This poses new challenges to maintain the robustness and resilience of the electricity grid.

Energy storage is one of the several potentially important technologies which will ease the integration challenges. Storage devices allow better coordination between electricity production and usage by shifting energy from periods of low demand to periods of high demand, thereby reducing curtailment. In addition, storage can provide a wide range of high value services, ranging from wholesale capacity for large power grids to back-up energy for individual consumer (see [1] for details).

The potential benefits of storage have spurred an interest in significant expansion of storage deployment. Based on available data ([2]), at least 185 GW of large scale storage is currently installed in electricity grids worldwide. While the majority (96%) of installation is pumped-storage hydro power, other technologies, such as, compressed air energy storage, flywheels, thermal storage and batteries, are gaining popularity. According to one estimate, an additional 310 GW of storage will be needed in four major regions (China, India, the European Union and the United States) by 2050 where 85% of global electricity demand will be concentrated (see [3]).

Charging storage devices during periods of low financial value and discharging when value is high, often referred to as energy arbitrage, is one of the most commonly studied storage applications ([4]). Analysis of energy arbitrage are based on deterministic optimization techniques using either perfect-foresight or historical prices which are assumed to repeat themselves (see for example [5] for New York ISO market and [6] for PJM market). The value of storage devices to provide both arbitrage as well as frequency regulation was studied in [7] (also using historical data). The role of storage devices in increasing the value of wind generation has been studied from a game-theoretic perspective in [8], and from a simulation perspective in [9].

The storage problem bears some resemblance to classical inventory management problems. Many researchers have employed Markov decision process (MDP) models, common in the supply-chain literature, to determine threshold storage policies [10], optimal bidding and storage strategies [11], and value of storage devices for energy arbitrage and ancillary services [12]. The computational approach adopted in these works (for, e.g., approximate dynamic programming) often resort to coarse discretization of states (renewable generation and/or storage level) or solve the sample average approximation problem to manage the inherent curse of dimensionality of MDP models. Storage commitment and utilization policies have been derived within the MDP setting under simplifying assumptions on distribution of renewable generation (for, e.g., [13]).

Coupling wind energy with storage has also been studied using stochastic programming (SP) techniques. A stochastic program in extensive form was used for the arbitrage problem using price scenarios in [14]. A similar approach was used in [15] to determine capacity of pumped hydro in a power system with large renewable penetration. In [16] the daily operations of a system with pumped hydro and wind power plants is modeled as a multistage stochastic program using a scenario tree representation of wind generation. In all these works the solution technique is limited to solving a single, large linear program. However, solving linear programs, even with a modest number of scenarios, may prove to be unwieldy for real scale power networks, as shown in our previous work [17]. An exception to such extensive form stochastic linear programs is the spark-spread optimization model presented in forward-contract planning in [18].

A common SP approach employed is to model the problem, for example, the robust unit-commitment problem with pumped-storage units in [19] and storage sizing problem in [20], as a two-stage stochastic program. These approaches use Benders decomposition as the solution methodology. Although these SP models allow for the incorporation of realistic constraints, they limit the number of scenarios used for optimization so that tractability can be achieved. Moreover, these schemes require *a priori* selection of scenarios and an explicit knowledge of their probability distribution. However, choosing a set of "good" scenarios and associating them with the "right" distribution is often difficult, particularly for uncertain parameters like intermittent generation and demand [17]. To overcome this, systems such as numerical weather prediction (NWP) [21] can be used to produce forecasts that simulate the behavior of the atmosphere extremely well. These systems are based on observations of physical attributes like temperature, radiation, humidity etc. They use data assimilation techniques and numerical computer models to generate multiple versions of the forecast from slightly different initial states which provide an accurate and reliable estimate of uncertainty. To harness these merits we need a framework which can directly use these forecasts within an optimization algorithm.

In this paper we consider short-duration storage devices (lasting a few minutes), which have the potential to ease the integration of intermittent resources in a power system [22].

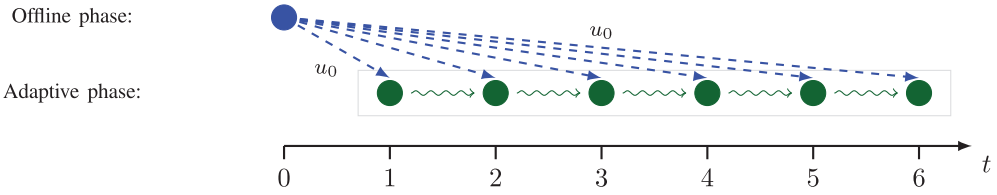

Fig. 1. Timescales and system dynamics ($T = 6$).

The MDP and SP models mentioned earlier consider a single (often grid-level) storage device. Unlike these models, our setup allows storage devices which can be connected to different buses in the network, and hence our use of the term "distributed storage". This setup is based on multistage stochastic programming, and incorporates power flow constraints and operating reserves, along with conventional and renewable generation. In systems with significant renewable energy and storage devices, large thermal generators need to be controlled at coarse timescale to accommodate their physical limitations (ramping constraints). Note that, fine timescale fluctuations in demand and intermittent generation are handled by load-following reserves and short-duration storage devices. This leads to a two-scale stochastic decision process. Moreover, storage devices link the state of the system from one time period to the next, and hence we have a sequential decision process at fine timescale. For such systems a suitable model is necessary to capture their two-scale stochastic decision processes. In this regard, the main contributions are:

- *Two-scale Model for Distributed Storage Control:* We consider a power system which consists of conventional as well as renewable energy resources. To address the non-dispatchability of renewable resources, we consider distributed storage devices. These resources are accommodated in a model which captures decisions at two levels of granularity. The fine timescale is an adaptive phase where the system responds to data that will be revealed at higher frequency. The coarse timescale, on the other hand, is more strategic and decisions are made prior to observing fine timescale data. To the best of our knowledge, this is the first application of multistage stochastic programming for distributed storage control in power systems.
- *Optimization and Simulation:* We allow state-of-the-art simulators to produce high frequency data which is directly available for use within optimization algorithm. Such simulators mimic system evolution in a manner that has typically been validated by power system experts. By the same token, our setup permits historical data to be directly imported into stochastic optimization. This setup is described in Section III.
- *Scalability:* Computational experiments that show that our algorithm provides solutions and objective function values which are statistically indistinguishable from results obtained from SDDP while significantly reducing the computational requirement. These results are presented in Section IV. Such speed-ups are critical for applying stochastic optimization algorithms for large scale system such as those encountered in power systems. This paper provides the first computational evidence in this regard.

II. Model Formulation

We consider a model in which the decision maker is required to make an "offline" decision which corresponds to conventional generation. This decision influences the system operations over multiple fine timescale periods where corrective actions can be taken in an adaptive manner. These fine timescale decisions correspond to utilization of the power network, operating reserves, storage devices and renewable energy resources. Hence the model comprises of an offline phase and an adaptive phase. In our formulation we will use $t = 0$ to index the offline decision epoch, and the set $\mathcal{T} := \{1, 2, \ldots, T\}$ will denote the adaptive decision epochs. Figure 1 presents a pictorial representation of this decision process.

A. Short-Term Storage Control Model

Let $\mathcal{B}$ denote the set of buses and $\mathcal{L}$ the set of links in a power grid. The grid comprises of energy resources which include conventional slow-ramping generators $\mathcal{G}$, fast-ramping operating reserves $\mathcal{R}$ and renewable resources $\mathcal{W}$. In addition to these, the grid also consists of distributed storage devices which are indexed by the set $\mathcal{N}$. These resources together serve demand at locations indexed by set $\mathcal{D}$.

1) Offline/Coarse Timescale Problem: At the coarse timescale, the decisions u_0 consists of generation levels G_i for slow-ramping generators, i.e., $u_0 := (G_i)_{\forall i \in \mathcal{G}}$. The generators are limited by their capacity and ramping capability. Given the initial generation levels $(G_i^{init})_{i \in \mathcal{G}}$, these limitations are captured by the following constraints:

$$\mathcal{U}_0 := \left\{ G_i \middle| \begin{array}{l} G_i^{min} \leq G_i \leq G_i^{max} \\ \Delta G_i^{down} \leq G_i - G_i^{init} \leq \Delta G_i^{up} \end{array} \right\}_{\forall i \in \mathcal{G}}. \quad (1)$$

Here $[G_i^{min}, G_i^{max}]$ are capacity limits, ΔG_i^{down} is maximum down-ramp capability and ΔG_i^{up} is up-ramp capability of generator $i \in \mathcal{G}$.

The objective of the course timescale problem is to minimize the sum of total production cost and an expected recourse function:

$$\min \sum_{i \in \mathcal{G}} d_i^{gen} G_i + \mathbb{E}[h_1(\tilde{s}_1)], \quad (2)$$

where d_i^{gen} is the unit production cost of generator i which depends on heat rate, fuel type and unit price of fuel used by the generator. Here, $\tilde{s}_1$ is a random variable which denotes the system state, which we define next.

2) System Dynamics: The dynamics underlying our model captures the relationship between decisions and data in the adaptive phase, viz. energy stored in the distributed storage resources, operating reserve utilization and renewable generation. In order to capture this dynamics, the system is represented by a state variable $s_t := (u_0, x_t, \omega_t)$. A realization of this state variable constitutes the following: the offline decision u_0, an endogenous state x_t which can be controlled by an adaptive phase algorithm, and the exogenous information ω_t over which the decision maker cannot exert any control.

As data is revealed over time, some of the dependence of variables on future data can only be captured probabilistically. To indicate this in our formulation, we will use $\tilde{s}_{t+} = (u_0, \tilde{x}_{t+}, \tilde{\omega}_{t+})$ to denote random quantities observed in the future.

In our model, exogenous information at time period t is a vector of renewable generation: $\tilde{\omega}_t = (\widetilde{W}_{it})_{i\in\mathcal{W}}$. A vector corresponding to energy stored in storage devices $(x_{it}^{store})_{i\in\mathcal{N}}$ and operating reserve utilization level $(x_{it}^{res})_{i\in\mathcal{R}}$ will constitute the endogenous state.

We consider the storage resources to be highly responsive short duration devices capable of providing regulation services. These devices are connected to different buses in the network, and are indexed by the set $\mathcal{N}$. They are characterized by:

- V_i^{max} = storage capacity,
- ΔV_i^+, ΔV_i^- = power rating that specifies the rate at which storage can be charged or discharged respectively,
- ρ_i^+, ρ_i^- = efficiency which accounts for conversion losses during charging and discharging respectively, and
- η = dissipation losses due to leakages,

for all $i \in \mathcal{N}$. Note that $0 < (\rho_i^+\rho_i^-) \leq 1$, where $(\rho_i^+\rho_i^-)$ denotes the round-trip efficiency. These parameters are assumed to be input to our model.

The storage level x_{it} in device $i \in \mathcal{N}$ evolves under the influence of charging (ν_{it}^+) and discharging (ν_{it}^-) decisions according to:

$$\tilde{x}_{it+}^{store} = \eta_i x_{it}^{store} + \rho_i^+ \nu_{it}^+ - \rho_i^- \nu_{it}^-. \tag{3}$$

Similarly, the state of operating reserves is determined by decision r_{it} which can be captured by the following relationship:

$$\tilde{x}_{it+}^{res} = r_{it} \quad \forall i \in \mathcal{R}. \tag{4}$$

The decisions ν_{it}^+, ν_{it}^- and r_{it} depend on the renewable generation data revealed in the interval $(t, t+1]$ (a random variable). Therefore, the energy stored in these devices $(\tilde{x}_{t+}^{store} = (\tilde{x}_{it}^{store})_{i\in\mathcal{N}})$ and the state of operating reserves $(\tilde{x}_{t+}^{res} = (\tilde{x}_{it+})_{i\in\mathcal{R}})$ in time period $t+$ are also a random variables.

Let A_t be a diagonal matrix with η_i as the ith diagonal element. Let $B_t = [B_t^{store}, B_t^{res}]^\top$, where B_t^{store} is a matrix with ρ_i^+ and ρ_i^- as ith row elements corresponding to ν_{it}^+ and ν_{it}^- columns respectively, and B_t^{res} is a matrix with entry equal to one corresponding to r_{it} columns. Using these matrices we can write the evolution in (3) and (4) as the following stochastic linear dynamics:

$$x_{t+} = \begin{cases} A_{t+}x_t, & \text{if } t = 0, \\ A_{t+}x_t + B_{t+}u_t & \text{if } t \in \mathcal{T} \setminus T \end{cases} \tag{5}$$

where x_0, which corresponds to the initial storage level and state of operating reserves, is assumed to be given.

3) Exogenous Process: Renewable generation at all locations $i \in \mathcal{W}$ can be described as stochastic processes which exhibit temporal and spatial correlation. Autoregression based time series models have been used to represent these stochastic processes. For example, in [23] univariate modeling procedures were applied on historical data for individual wind farms and a covariance matrix of error terms was estimated separately to describe spatial correlation, and alternatively in [24] multivariate models were employed. A m-th order multivariate autoregressive process can be represented in matrix form (see [25] for details) as:

$$\text{VAR}(m) : \omega_{t+} = \sum_{j=1}^{m} \Phi_j \omega_{t-j+1} + \epsilon_{t+} \quad \forall n, \tag{6}$$

where ϵ_t is a $|\mathcal{W}|$ dimensional white noise process with time invariant positive definite covariance matrix ($\mathbb{E}[\epsilon_t] = 0; \mathbb{E}[\epsilon_t\epsilon_t'] = \Sigma_\epsilon; \mathbb{E}[\epsilon_n\epsilon_{n'}]_{n\neq n'} = 0$) and $(\Phi_j)_{j=1}^m$ are autoregression coefficient matrices.

Note that, by appropriately appending the endogenous state variable x_t by past observations $(\omega_j)_{j=t-m+1}^t$ and matrix A_{t+} by coefficient matrices $(\Phi_j)_{j=1}^m$, the VAR(m) model can be subsumed into the stochastic linear dynamics of (5). In this case, the uncertainty is confined to random noise process $\{\epsilon_t\}$ which exhibits stagewise independence.

4) Adaptive/Fine Timescale Problems: The fine timescale problems address economic dispatch of generation to meet demand in the network for all $t \in \mathcal{T}$. In case of excess (or insufficient) generation, the grid is allowed to sell (or buy) energy from neighboring grids through a set of intertie nodes $\mathcal{I}$. The amount of energy bought and sold at bus $i \in \mathcal{I}$ is denoted by q_{it}^+ and q_{it}^-, and the corresponding costs are denoted by d_{it}^{buy} and d_{it}^{sell} respectively.

At each bus $i \in \mathcal{B}$ in the network, the power flow equation ensure that energy is conserved. These equations are given by:

$$\sum_{j:(j,i)\in\mathcal{L}} p_{jit} - \sum_{j:(i,j)\in\mathcal{L}} p_{ijt} + \sum_{j\in\mathcal{R}_i} r_{jt} + \sum_{j\in\mathcal{W}_i} \left(\nu_{it}^- - \nu_{it}^+\right) + \sum_{j\in\mathcal{I}_i} \left(q_{jt}^+ - q_{jt}^-\right) = \sum_{j\in\mathcal{D}_i} D_{jt} - \sum_{j\in\mathcal{W}_i} \widetilde{W}_{jt} - \sum_{j\in\mathcal{G}_i} G_j. \tag{7}$$

Here D_{it} denotes demand at $i \in \mathcal{D}$, r_{it} the reserve utilization for $i \in \mathcal{R}$ and p_{ijt} the power flow on line $(i,j) \in \mathcal{L}$. Flow in power networks are inherently alternating (AC) in nature and therefore, physical quantities involved (such as active power, reactive power, and magnitude of voltages) are non-linear. This yields an optimal power flow problem which is non-convex and, in general, is hard to solve. Recent studies, for, e.g., [26], provide techniques for convex relaxation of these problems which are then solved using semi-definite programming. However, inclusion of AC power flows in current setting results in a stochastic semi-definite program and current stochastic optimization algorithms are inadequate to handle these due to the associated computational difficulty. Therefore, in most power systems of realistic size, power flow is represented using second-order approximations, leading to linear constraints. In the interest of scalability, our paper also

adopts this approach. Power flows on line $(i,j) \in \mathcal{L}$ is captured by the following equation:

$$p_{ijt} = \frac{\Lambda_i \Lambda_j}{X_{ij}}\left(\theta_{it} - \theta_{jt}\right) \qquad \forall (i,j) \in \mathcal{L}, \tag{8}$$

where Λ_i is the bus voltage and θ_{ti} is the phase angle at $i \in \mathcal{B}$, while X_{ij} is the reactance of line $(i,j) \in \mathcal{L}$.

The physical limits of transmission lines and the second-order approximation on power flows enforce the following bounds:

$$p_{ij}^{min} \le p_{ijt} \le p_{ij}^{max} \qquad \forall (i,j) \in \mathcal{L} \tag{9a}$$

$$\theta_i^{min} \le \theta_{it} \le \theta_i^{max} \qquad \forall i \in \mathcal{B}. \tag{9b}$$

As with slow-ramping generators, the operating reserves are also constrained by their capacity (R_i^{min}, R_i^{max}) and ramping capability $(\Delta R_i^{down}, \Delta R_i^{up})$ as follows:

$$R_i^{min} \le r_{it} \le R_i^{max}, \tag{10a}$$

$$\Delta R_i^{down} \le r_{it} - x_{it}^{res} \le \Delta R_i^{up} \qquad \forall i \in \mathcal{R}. \tag{10b}$$

The total amount of energy stored in storage devices is limited by their capacity. The power rating of the device imposes a bound on charging and discharging decision variables. These restrictions for $i \in \mathcal{N}$ are captured by the following constraints:

$$0 \le x_{it} + \nu_{it}^{+} - \nu_{it}^{-} \le V_i^{max} \tag{11a}$$

$$0 \le \nu_{it}^{+} \le \Delta V_i^{+}; \quad 0 \le \nu_{it}^{-} \le \Delta V_i^{-}. \tag{11b}$$

The cost incurred in adaptive phase is due to usage of storage devices, generation from operating reserves and transaction with other grids. The unit production cost for operating reserve $i \in \mathcal{R}$ is denoted by d_i^{res} and the unit storage cost is denoted by c_{it}^{store} for $i \in \mathcal{N}$. We choose the transaction costs such that $d_i^{buy} \gg d_i^{sell}$. This avoids overgeneration in the grid in order to profit by selling to other grids. The stagewise objective function can be stated as follows:

$$h_t(s_t) = \sum_{i \in \mathcal{N}} c_{it}^{store} x_{it}^{store} + \min \sum_{i \in \mathcal{R}} d_i^{res} r_{it} + \sum_{i \in \mathcal{I}} \left(d_{it}^{buy} q_{it}^{+} - d_{it}^{sell} q_{it}^{-} \right) + \mathbb{E}[h_{t+}(\tilde{s}_{t+})]. \tag{12}$$

To summarize, the fine timescale decision vector u_t includes $(p_{ijt})_{(i,j)\in\mathcal{L}}$, $(\theta_{it})_{i\in\mathcal{B}}$, $(r_{it})_{i\in\mathcal{O}}$, $(\nu_{it}^{+}, \nu_{it}^{-})_{i\in\mathcal{W}}$ and $(q_{it}^{+}, q_{it}^{-})_{i\in\mathcal{I}}$, and the feasible set $\mathcal{U}_t(s_t)$ is characterized by constraints (7)-(11). Note that the feasible set is parameterized by s_t which includes the offline decisions $(G_i)_{i\in\mathcal{G}}$, endogenous state $((x_{it}^{store})_{i\in\mathcal{W}}, (x_{it}^{res})_{i\in\mathcal{R}})$ and exogenous information $(\widetilde{W}_{it})_{i\in\mathcal{W}}$.

B. Mathematical Structure

The decision process described above can succinctly be represented as a multistage stochastic linear program (MSLP). The process starts by identifying the offline decision vector $u_0 \in \mathcal{U}_0$. This decision is made before any uncertainty is realized, and is obtained by solving the following optimization problem:

$$h_0(x_0) = c_0^{\top} x_0 + \min \; d_0^{\top} u_0 + \mathbb{E}[h_{0+}(\tilde{s}_{0+})] \quad s.t. \; D_0 u_0 \le b_0(x_0). \tag{13}$$

Here, $h_{0+}(\tilde{s}_{0+})$ is the recourse function for adaptive phase corresponding to the offline decision u_0, endogenous state x_{0+} and a realization ω_{0+} of the random variable $\tilde{\omega}_{0+}$. When the exogenous information is revealed sequentially over $t \in \mathcal{T}$, this recourse function can be decomposed into stages which allows optimal decisions to be made at each $t \in \mathcal{T}$. This can be stated in a recursive form as follows:

$$h_t(s_t) = c_t^{\top} x_t + \min \quad d_t^{\top} u_t + \mathbb{E}[h_{t+}(\tilde{s}_{t+})] \quad s.t. \; D_t u_t \le b_t - C_t x_t - C_0 u_0, \tag{14}$$

where x_{t+} satisfies the dynamics in (5), and the terminal cost function $h_{T+}(s_{T+})$ is assumed to be given. At each stage, the decision depends only on information available at that time (i.e., s_t), but not on observations in later stages. This is known as the non-anticipativity requirement in stochastic programming literature [27]. Since the offline decision u_0 directly effects all the recourse problems in adaptive phase, we will refer to the model in (13)-(14) as two-scale multistage stochastic linear program (2-MSLP). The standard MSLP is a one-scale formulation where decisions at a particular stage have direct effect only on the subsequent stage.

The earliest applications of MSLP models have used algorithms which are multistage extensions of Benders' decomposition, for example, the Nested Decomposition method proposed in [28]. Other methods include the scenario decomposition method of [29], and the progressive hedging algorithm by [30]. A common feature across all these algorithms is the use of deterministic approximation of uncertainty through scenario trees which are generated using techniques like those proposed in [31]. When the underlying stochastic process becomes complicated, their deterministic approximation may result in large unwieldy scenario trees, and one may have to resort to scenario reduction methods (e.g., [32]) to achieve computational viability.

The more successful approaches in practical applications appear to be the sampling-based methods, and in particular, the stochastic dual dynamic programming (SDDP) algorithm. The SDDP setting provides a computationally viable platform to deal with detailed models with many realistic considerations, especially with respect to scheduling hydro-electric reservoirs [33]. Lately, several commercial implementations of SDDP have also emerged and are being used for planning power systems operations in a number of South American countries (see [34] and references therein). Like MSLP algorithms mentioned earlier, SDDP creates outer approximation of the value function using subgradient information. However, it avoids intractability of scenario trees by assuming stagewise independent uncertainty. While the algorithm traverses forward using sampling, the approximations are created on the backward pass from deterministic Benders' cuts based on subgradients generated using all possible outcomes in a particular stage. The interstage independence assumption allows these cuts to be shared across different states within a stage. Cut sharing under special stagewise dependency as presented by [35], the algorithmic enhancements proposed in [36], and the inclusion of risk measures [37] have contributed to the

success of SDDP. Due to these reasons, as well as its success in controlling reservoir storage in hydro-electric power systems, we will use SDDP for benchmarking our algorithm in the computational study.

In most stochastic programming algorithms, scenarios are generated (whether by selection, sampling or scenario reduction) prior to the optimization phase. Due to this sequence of steps, the optimization algorithm is unable to verify the introduction of bias within the context of scenarios that are provided. The sequential sampling technique adopted in our work allows us to use an unbiased estimator (sample mean function) to approximate the expectation function. This technique provides two principal advantages (a) it enables our algorithm to be applicable for problems where the underlying probability is unknown, and (b) it provides the means to design statistical stopping rules. The reader is referred to [38] for both the theory and computational results supporting this advantage.

III. Algorithm

We present a sequential sampling algorithm in this section which we call the two-scale stochastic dynamic linear programming (2-SDLP). The algorithm was originally designed for state-variable formulation of MSLPs in [39], and has been modified to accommodate the two-scale nature of the formulation considered in this paper.

It is well known that the expected recourse function in (13) and (14) are piecewise linear and convex in decision variables (Chapter-3 in [27]). In algorithms like SDDP, an approximation of the recourse function is developed using subgradients obtained by solving a subproblem corresponding to every outcome of random variable $\tilde{\omega}_t$ at a stage. As expected, the computational requirement of such a procedure increases significantly with the number of outcomes. We overcome this concern by developing approximations based on statistical estimates of the recourse function. In addition to computational gains, our approach avoids the need for *a priori* knowledge of probability distribution. We will present the main steps of the algorithm here, and refer the reader to [39] and [40] for a detailed description and analysis. Algorithms of this type are generalization of stochastic subgradient methods [41], [42], with the differences arising from the fact that our approach uses a bundle of sample mean approximations. Such methods are essentially online (or incremental sampling algorithms) for MSLP models which are convex optimization problems.

Our algorithm is applicable to problems in which the set of offline decisions is closed and bounded. Moreover, the SP model itself is assumed to satisfy fixed and relatively complete recourse [27] in adaptive phase, and exogenous information which exhibits interstage independence. In our formulation the recourse matrix (which corresponds to the physical structure of power network) is fixed, and energy imbalance is mitigated by transactions with the neighboring grids, thereby satisfying complete recourse. Finally, the exogenous process considered in our model (see Section II-A3) satisfies interstage independence.

The algorithm works in two principal steps: (a) forward recursion during which decisions are simulated along a sample path, and (b) backward recursion when approximations for cost-to-go functions are updated. We will present the algorithm in iteration-k when approximations f_t^{k-1} of cost-to-go function are available for all non-terminal stages (i.e., $t \in \mathcal{T} \setminus T$). A schematic representation of the algorithm is presented in Figure 2.

A. Forward Recursion

In kth iteration of the algorithm, the forward recursion begins by identifying an offline decision u_0^k. This is followed by generating an observation of exogenous information $\{\omega_t^k\}$ over entire adaptive horizon $t = 1, \ldots, T$. This observation, or sample path, is generated independently of all previous observations.

Since we do not assume any knowledge of the exogenous information process, an estimation of the distribution is also approximated as the algorithm proceeds. In order to do this, let Ω_t^{k-1} denote the set of observations at time-t in the first $k-1$ iterations of the algorithm. The observation along the current sample path is added to this list to obtain the updated set: $\Omega_t^k = \Omega_t^{k-1} \cup \omega_t^k$. Further, the number of times a particular observation $\omega \in \Omega_t^k$ is encountered is updated as $\kappa_\omega^k = \kappa_\omega^{k-1} + 1_{\omega=\omega_t^k}$ to set up the empirical frequency $p_\omega^k = \kappa_\omega^k / k$.

Within our algorithm, we use the notion of "incumbent decisions". These incumbent decisions represent the best solutions identified by the algorithm in the first $k-1$ iterations. In order to comply with the non-anticipativity requirement of multistage stochastic programs these incumbent decisions are dependent on sample paths, and are denoted as $\hat{u}_t^{k-1}(\omega_t^k)$. Using these incumbent and current approximations, the forward pass decisions are obtained by solving:

$$u_t^k \in \underset{u_t \in \mathcal{U}_t(s_t^k)}{\arg\min} \left\{ f_t^{k-1}\left(u_t, s_t^k\right) + \frac{\sigma_t^k}{2} \left\| u_t - \hat{u}_t^{k-1}\left(\omega_t^k\right) \right\|^2 \right\}. \quad (15)$$

Here, the proximal parameter σ_t^k is assumed to be given. We will refer to these decisions as "candidate decisions" and the corresponding state s_t^k as the candidate state. Using the candidate decision u_t^k and sample observation ω_t^k in (5) we obtain the subsequent candidate state s_{t+}^k. This procedure is carried out recursively for all non-terminal stages $t \in \mathcal{T} \setminus T$. As in the case of regularized Benders [43] and 2-SD [44], the proximal term in the non-terminal stage problem objective function helps in stabilizing the algorithm and allows for the *a priori* specification of a fixed number of lower bounding affine functions to be used during the course of the algorithm. With this, the forward recursion procedure of iteration-k is complete.

B. Backward Recursion

As the name suggests these calculations are carried out backwards in time, starting from the terminal stage T to the offline stage, and along the same sample path observed during forward pass. The goal of backward recursion is to update the approximations of cost-to-go functions. At any stage, these updates are based on the empirical frequencies

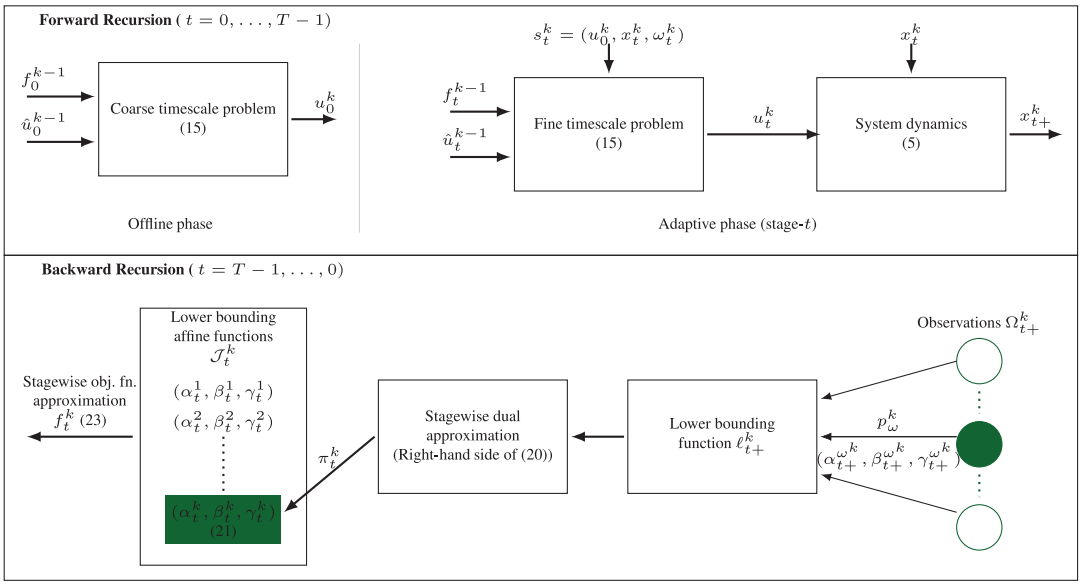

Fig. 2. Schematic representation of 2-SDLP.

p_ω^k for $\omega \in \Omega_t^k$ which are estimates of the unconditional probabilities of exogenous information at stage-t.

1) Terminal Stage Approximation: For terminal stage, recall that $\mathbb{E}[h_{T+}(s_{T+})] = 0$, and the cost-to-go function h_T is the value of a deterministic linear program. Therefore, the sample mean

$$H_T^k(u_0, x_{T-1}, u_{T-1}) = \sum_{\omega \in \Omega_T^k} p_\omega^k h_T\big(u_0, x_T^\omega\big) \tag{16}$$

provides an unbiased estimate of $\mathbb{E}[h_T(\tilde{s}_T)]$, where $x_T^\omega = \omega + A_T x_{T-1} + B_T u_{T-1}$. For the current offline decision u_0^k and candidate state $x_T^k = \omega_T^k + A_T x_{T-1}^k + B_T u_{T-1}^k$, we solve the recourse linear program in (14) and obtain the optimal dual solution π_T^k. Using linear programming duality we generate a lower bounding affine function as:

$$h_T(u_0, x_T) \geq \underbrace{c_T^\top x_T + \Big(\pi_T^k\Big)^\top [b_T - C_T x_T - C_0 u_0]}_{= \alpha_T^{\omega_T^k k} + \beta_T^{\omega_T^k k} x_T + \gamma_T^{\omega_T^k k} u_0} \tag{17}$$

This affine function is added to collection $\mathcal{J}_T^{k-1}$ of previously generated affine functions: $\mathcal{J}_T^k = \mathcal{J}_T^{k-1} \cup (\alpha_T^{\omega_T^k k}, \beta_T^{\omega_T^k k}, \gamma_T^{\omega_T^k k})$. For other observations $\omega \in \Omega_T^k$ $(\omega \neq \omega_t^k)$ the best lower bounding affine function from the collection $\mathcal{J}_T^k$ is identified as

$$\Big(\alpha_T^{\omega k}, \beta_T^{\omega k}, \gamma_T^{\omega k}\Big) \in \underset{(\alpha_T, \beta_T, \gamma_T) \in \mathcal{J}_T^k}{\arg\max} \Big\{\alpha_T + \beta_T x_T^{\omega k} + \gamma_T u_0^k\Big\} \tag{18}$$

We use $\{(\alpha_T^{\omega k}, \beta_T^{\omega k}, \gamma_T^{\omega k})\}_{\omega \in \Omega_T^k}$ to generate a lower bounding function to sample mean function in (16) as:

$$\begin{aligned} H_T^k(u_0, x_{T-1}, u_{T-1}) &\geq \sum_{\omega \in \Omega_T^k} p_\omega^k \Big[\alpha_T^{\omega k} + \beta_T^{\omega k} x_T^\omega + \gamma_T^{\omega k} u_0\Big] \\ &= \ell_T^k(u_0, x_{T-1}, u_{T-1}). \end{aligned} \tag{19}$$

2) Non-Terminal Stage Approximation: Consider the non-terminal stage t. For this stage we approximate the expected recourse function in (14) using a sample mean function (similar to (16)). Since we proceed backwards in time, we have access to an affine lower bounding function $l_{t+}^k(u_0, x_t, u_t) = \sum_{\omega \in \Omega_{t+}^k} p_\omega^k [\alpha_{t+}^{\omega k} + \beta_{t+}^{\omega k} x_{t+}^\omega + \gamma_{t+}^{\omega k} u_0]$ to the sample mean. Using this we can setup an approximate stage problem as follows:

$$\begin{aligned} h_t^k(s_t) &= c_t^\top x_t + \min_{u_t \in \mathcal{U}_t(s_t)} \; d_t^\top u_t + H_{t+}^k(u_0, x_t, u_t) \\ &\geq c_t^\top x_t + \min_{u_t \in \mathcal{U}_t(s_t)} \; d_t^\top u_t + \ell_{t+}^k(u_0, x_t, u_t). \end{aligned} \tag{20}$$

Let π_t^k be the optimal dual solution obtained by solving the linear program on the right-hand side of (20) with s_t^k as input. Using this dual solution, the definition of ℓ_{t+}^k and the constraint set $\mathcal{U}_t(s_t)$ we compute a lower bounding affine function similar to (17) with coefficients (see [39] for details):

$$\alpha_t^k = \Big(\pi_t^k\Big)^\top b_t + \sum_{\omega \in \Omega_{t+}^k} p_\omega^k \alpha_{t+}^{\omega k}, \tag{21a}$$

$$\beta_t^k = c_t - C_t^\top \pi_t^k + \sum_{\omega \in \Omega_{t+}^k} p_\omega^k \Big(\beta_{t+}^{\omega k}\Big)^\top A_{t+}, \tag{21b}$$

$$\gamma_t^k = -C_0^\top \pi_t^k + \sum_{\omega \in \Omega_{t+}^k} p_\omega^k \gamma_{t+}^{\omega k}. \tag{21c}$$

The coefficients above are similar to those used in (18).

As before, this affine function is added to the collection $\mathcal{J}_t^{k-1}$, and for observations $\omega \neq \omega_t^k$ the coefficients of the best lower bounding function $\{(\alpha_t^{\omega k}, \beta_t^{\omega k}, \gamma_t^{\omega k})\}_{\omega \in \Omega_t^k}$ are obtained from the collection $\mathcal{J}_t^k$ as in (18). Using these coefficients we obtain a lower bound on the sample mean function for stage-t:

$$\begin{aligned} H_t^k(u_0, x_{t-1}, u_{t-1}) &\geq \sum_{\omega \in \Omega_t^k} p_\omega^k \Big[\alpha_t^{\omega k} + \beta_t^{\omega k} x_t^\omega + \gamma_t^{\omega k} u_0\Big] \\ &= \ell_t^k(u_0, x_{t-1}, u_{t-1}) \end{aligned} \tag{22}$$

where, $x_t^\omega = \omega + A_t x_{t-1} + B_t u_{t-1}$.

TABLE I
DETAILS OF TEST SYSTEMS AND PROBLEM SIZES

System	Buses	Lines	Thermal	Wind	Offline phase		Adaptive phase (per stage)				
					Rows	Columns	Rows	Columns	Random Variables	Outcomes	Storage Devices
IEEE-14	14	20	5	1	10	5	36	39	1	5	1
IEEE-30	30	41	6	3	12	6	75	80	3	125	3
IEEE-57	57	80	7	5	14	7	143	150	5	3125	5
IEEE-118	118	186	46	8	92	46	363	582	8	Simulator outputs	5

The affine functions in (19) and (22) lower bound their corresponding sample mean functions. As the algorithm proceeds, the probability estimates (p^k_ω) used to set up these sample means get updated, and even the number of observations in Ω^k_t increases with every new sample encountered. In order to ensure that the affine functions generated at iteration-$j < k$ continue to lower bound the sample mean in iteration-k, they need to be re-adjusted. If we assume, without loss of generality, that $h_t \geq 0$, the readjustment can be performed by multiplying the previously generated affine functions by a factor of (j/k). With these updated affine functions the approximate stagewise objective function for $t \in \mathcal{T} \setminus T$ is given by:

$$f^k_t(u_t, s_t) = d_t^\top u_t + \max_{j=1,\ldots,k} \left\{ \frac{j}{k}\ \ell^j_{t+}(u_0, x_t, u_t) \right\} \tag{23}$$

The backward recursion is completed by updating the incumbent solutions along the current sample path. These updates are carried out in time order, starting from offline stage, and are based on predicted objective value reduction at the root stage:

$$f^k_0\left(u^k_t, s_0\right) - f^k_0\left(\hat{u}^{k-1}_0, s_0\right) \leq q\left[f^{k-1}_0\left(u^k_0, s_0\right) - f^{k-1}_0\left(\hat{u}^{k-1}_0, s_0\right)\right]. \tag{24}$$

Here $q \in (0, 1)$ is a given parameter. If the above inequality is satisfied then the candidate decision is set as the incumbent decision for the current sample path. That is, $\hat{u}^k_t(\omega^k_t) = u^k_t$ for all $t \in \mathcal{T} \setminus T$. On the other hand, if the inequality is not satisfied, then the current incumbent solutions are retained ($\hat{u}^k_t(\omega^k_t) = \hat{u}^{k-1}_t(\omega^k_t)$). These updates are carried out only along the current sample path, while the incumbent decisions along other paths are retained. This update rule is similar to incumbent updates carried out in non-smooth optimization methods including regularized 2-SD [44] and MSD [39].

IV. COMPUTATIONAL RESULTS

In order to examine the computational performance of 2-SDLP algorithm, we conduct experiments on four IEEE test systems obtained from [45]. These networks are modified to include wind generation and storage devices. Table I presents the details of these test systems and size of the problems with two-scale MSLP formulation with a single offline decision vector and an adaptive phase with six stages. For our computational runs, we assume that all thermal generators in the system are committed and switched on. We will use smaller test instances to compare our 2-SDLP algorithm with the benchmark SDDP algorithm, and then provide results for a more realistic setting, which combines optimization and simulation, with larger instances.

The smaller test instances were built for IEEE-14, -30, and -57 systems. These instances were created by setting the renewable penetration level to 10% and varying the renewable generation trend over the time horizon (positive-p, negative-n and zero-z). The number of storage devices in each of these systems is shown in Table I. In these instances, the storage devices are assumed to be co-located with renewable generators, have a uniform capacity of 50 MW, round trip efficiency of one, and no dissipation loss.

The SDDP algorithm of [36] was modified to accommodate the two-scale structure of the problem considered here. The exogenous observations are discretized *a priori* and their empirical distribution is used to create approximation within the SDDP algorithm. To maintain consistency, a simulator with identical probability distribution is used to generate sample paths for 2-SDLP algorithm.

All experiments were carried out on a 64-bit Intel-core i7-2600 CPU @3.4GHz × 8 machine with 4 GB memory. Both algorithms were implemented in the C programming language, and all linear and quadratic programs were solved using CPLEX callable subroutines.

1) Comparison of Value Functions: Here, we compare the prediction values of the offline-phase generated by 2-SDLP with those obtained from SDDP. Both the algorithms were run for a fixed number of iterations using scenarios generated from the same seed. Prediction values at the end of 1000 iterations are presented as v_1 and v_2 in Table II for SDDP and 2-SDLP, respectively. The table also presents the estimated upper bound obtained by simulating SDDP decisions along scenarios (generated independently of those used during optimization) and computing the cost associated with them. Table II presents the mean, standard deviation and the 95% confidence interval (C.I.) of estimated upper bound. The results indicate that the difference between the upper confidence bound and the prediction value (which is the estimate of lower bound) is less than 0.005 for all the instances. This suggests that SDDP has solved the problem with a relative accuracy of 0.005 with probability 0.95 [46]. The last column of Table II indicates that the prediction value generated by 2-SDLP is within 0.2% of that predicted by our benchmark SDDP algorithm. Therefore, we can conclude that both the algorithms provide reliable cost estimates for our distributed storage control problem.

TABLE II
COMPARISON OF ESTIMATED VALUES BETWEEN THE SDDP AND 2-SDLP

Instances	SDDP						2-SDLP		Difference
	Time per iter.	Prediction value (v_1)	U.B. Estimation Mean	Std. dev.	95 % C.I. $[CI_\ell, CI_u]$	$\frac{CI_u - v_1}{v_1}$	Time per iter.	Prediction value(v_2)	$\frac{\lvert v_2 - v_1 \rvert}{v_1}$
ieee14n	0.001	6534.47	6535.76	2.60	[6530.67,6540.86]	0.0009	0.020	6537.89	5e-4
ieee14z	0.001	6353.72	6351.59	2.72	[6346.25,6356.93]	0.0008	0.021	6353.72	3e-4
ieee14p	0.001	5991.30	5992.64	2.72	[5987.30,5997.98]	0.0011	0.023	5994.77	6e-4
ieee30n	0.070	8489.47	8487.38	8.77	[8470.19,8504.58]	0.0017	0.052	8482.08	8e-4
ieee30z	0.025	7804.19	7801.54	6.26	[7789.26,7813.82]	0.0012	0.042	7786.69	2e-3
ieee30p	0.021	7334.09	7340.13	6.79	[7326.80,7353.46]	0.0026	0.038	7309.49	3e-3
ieee57n	1.023	24684.45	24695.83	4.75	[24686.51,24705.14]	0.0008	0.070	24639.42	2e-3
ieee57z	0.793	24279.30	24287.18	5.09	[24277.20,24297.16]	0.0007	0.076	24229.24	2e-3
ieee57p	0.641	22850.14	22868.82	4.58	[22849.84,22867.81]	0.0008	0.068	22854.57	2e-4

TABLE III
COMPARISON OF SOLUTIONS BETWEEN SDDP AND 2-SDLP

Instance	SDDP				2-SDLP				p-value
	Total Generation	Estimation Mean	Std. dev.	95 % C.I.	Total Generation	Estimation Mean	Std. dev.	95 % C.I.	
ieee14n	289.00	6535.76	2.68	[6528.25,6540.86]	289.00	6535.76	2.68	[6528.25,6538.74]	1.000
ieee14z	271.74	6348.72	2.79	[6343.24,6354.19]	271.74	6348.72	2.79	[6343.24,6354.19]	1.000
ieee14p	267.85	5989.76	2.79	[5984.29,5995.24]	267.85	5989.76	2.79	[5984.29,5995.24]	1.000
ieee30n	255.00	8487.38	8.77	[8470.19,8504.58]	255.00	8487.38	8.77	[8470.19,8504.58]	1.000
ieee30z	249.00	7747.33	4.58	[7738.36,7756.30]	248.90	7747.33	4.59	[7738.36,7756.30]	0.999
ieee30p	243.22	7319.11	6.68	[7306.02,7332.20]	242.67	7318.14	7.00	[7304.43,7331.85]	0.920
ieee57n	1149.2	24613.54	3.36	[24606.96,24620.13]	1151.7	24620.02	2.88	[24614.38,24625.67]	0.142
ieee57z	1068.5	24229.88	3.52	[24222.98,24236.78]	1069.4	24231.23	3.01	[24225.32, 24237.14]	0.770
ieee57p	1064.2	22848.72	4.41	[22840.08,22857.37]	1065.6	22848.89	3.79	[22841.47,22856.32]	0.977

Table II also presents the average time taken to complete an iteration of each algorithm. As the number of observations per stage increase from IEEE-14 to IEEE-57 system (see Table I), a greater number of linear programs are solved during backward pass of SDDP iteration, and therefore the time per iteration increases significantly. However in 2-SDLP, irrespective of number of observations per stage, only one linear program is solved in the backward pass of an SDDP iteration. The marginal increase in the time per iteration can be attributed to the increase in problem size.

2) Comparison of Offline-Phase Solution: We verify the similarity between offline decisions predicted by the two algorithms by evaluating them on the recourse problem corresponding to the complete adaptive phase:

$$\begin{aligned} h(u_0, \omega_{1:T}) = \min \; & \sum_{t=1}^{T} \left(c_t^\top x_t + d_t^\top u_t \right) \\ s.t. \; & C_t x_t + D_t u_t \leq b_t - C_0 u_0, \\ & x_{t+} = \omega_{t+} + A_{t+} x_t + B_{t+} u_t \quad \forall t. \end{aligned} \tag{25}$$

The offline decisions are fixed and scenarios are simulated from the same seed to set up the recourse problem. The process is terminated when a 95% C.I. is built on the objective function value. We test the following hypothesis: the offline solutions from the two algorithms are statistically indistinguishable. Table III presents the mean, standard deviation and the confidence interval from evaluation as well as the p-value associated with the hypothesis test. A p-value greater than 0.05 indicates that the hypothesis cannot be rejected at 0.95 significance level, moreover, a value of 1 indicates that the solutions are exactly the same. As the results show, the solutions from the two algorithms were either exactly the same or statistically indistinguishable for all instances tested in this experiment.

3) Optimization and Simulator: Optimization of power systems with significant renewable generation relies on an accurate representation of uncertainty. Simulation outcomes based on NWP models provide system operators with a means to achieve this. In this regard, we created instances of the larger IEEE-118 power system which directly use scenarios generated from a simulator for optimization. Experiments with these instances illustrate not only the scalability of our algorithm, but also its applicability in a more realistic setting. In these instances we have five storage devices (at buses 17, 37, 56, 77 and 92) which are not co-located with renewable generators. The round trip efficiency of current battery technology ranges between $70 - 85\%$ [47], and therefore we set $\rho_i^+ \rho_i^- = 0.8$ for all $i \in \mathcal{N}$. Further, the dissipation losses of storage devices increase with usage. We built instances with varying dissipation loss factor η_i to study its effect.

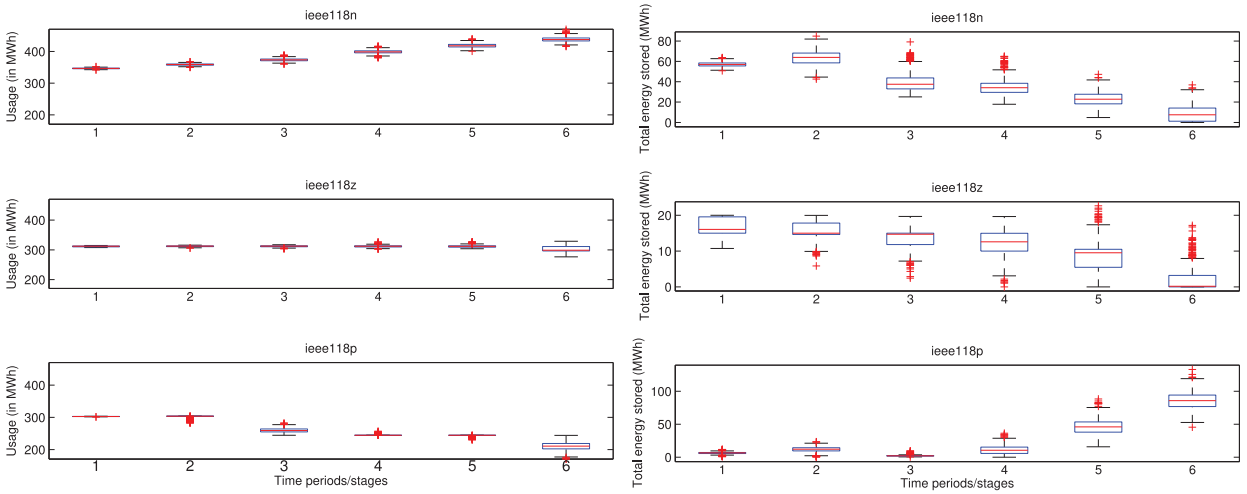

(a) Reserve utilization (b) Storage utilization

Fig. 3. Solutions for instances with varying trends.

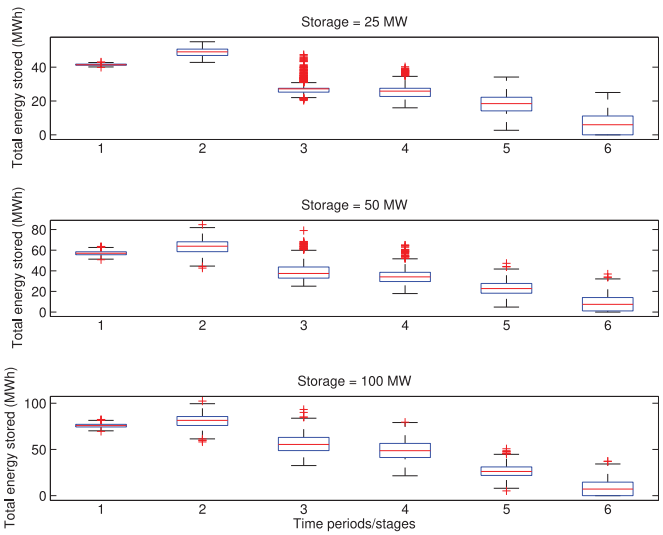

Fig. 4. Storage utilization in ieee118n instances.

As was the case earlier, different instances were created by selecting hours which exhibit different trends in renewable generation (positive-p, negative-n and zero-z), and varying the capacity of storage devices installed in the system (0, 50, 100 and 150 MW). For instances with varying storage capacity, an hour with negative trend in renewable generation was selected. The storage and reserve utilization results presented in Figure 3 and Figure 4 are obtained by fixing the coarse timescale decision and simulating the adaptive phase with a set of evaluation scenarios.

Our scenario simulations are based on the statistical model presented in (6) which is used as a proxy for NWP models. This model was designed using 2006 wind speed data for 8 wind farm locations chosen from the Western Wind and Solar Integration Study [48]. Based on the collected data, a VAR(2) model was selected for this experiment. We refer the reader to [23]–[25] for the necessary steps required for estimation of model parameters and their validation. Since the SDDP algorithm relies on *a-priori* knowledge of probability distribution, it is not compatible for use with a simulator. Therefore, the results in this subsection pertain only to the 2-SDLP algorithm.

TABLE IV
IEEE-118 RESULTS WITH SDLP-2

Instance	Storage Capacity	Time per iter.	Total Generation	Prediction Value
ieee118n	50	0.115	3800.2	1945692
ieee118z	50	0.116	3820.2	1707236
ieee118p	50	0.110	3780.3	1620306
ieee118n	0	0.110	3826.1	2008873
ieee118n	25	0.113	3798.1	1950388
ieee118n	50	0.115	3800.2	1945692
ieee118n	100	0.118	3798.7	1941083

From Figure 3a we observe that the amount of operating reserves utilized in ieee118n instance increases over time in order to compensate for the decrease in renewable generation. On the other hand, this utilization decreases for ieee118p instance. Moreover, the total amount of reserves utilized in ieee118n was, on an average, 49% higher than the ieee118p. While the conventional generation determined in the coarse stage is comparable for these two instances, the increase in reserve utilization results in higher total operating cost for ieee118n when compared to ieee118p (see prediction value in Table IV). The storage utilization results in Figure 3b indicate that there is greater value of storage devices in the early stages of negative trend instance when energy is stored for use during the later stages when the renewable generation decreases. In the instance with positive trend, however, the storage level increases only when renewable generation increases in later stages.

The presence of storage devices provides a buffer to overcome energy imbalance resulting from variability in renewable generation. This results is lower offline phase generation in the instance with even 25 MW storage capacity when compared to the instance with no storage (see Table IV). Moreover, an

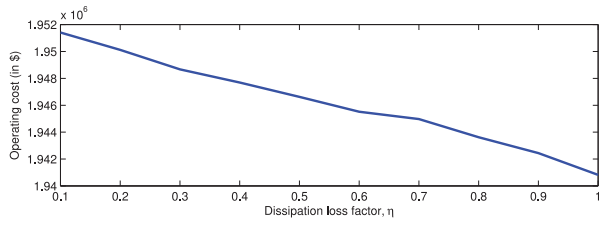

Fig. 5. Effect of dissipation loss on objective function value.

increase in storage capacity from 25 MW to 100 MW results in a reduction in operating reserve utilization. Due to these reasons, the total operating cost increases with decrease in storage capacity. The results in Figure 4 show the utilization of storage devices over model horizon. These results are for instances with a negative trend, and hence the storage levels decrease over the horizon.

The decrease in total operating cost when the trend changes from negative to positive was also observed in the smaller test instances. The behavior of operating reserves and storage devices was also similar in these instances. In addition, energy imbalance in the system was compensated by buying energy from the grid, which was higher in the initial stages of positive trend and the later stages of negative trend instances. On the other hand, our computational results do not indicate any correlation in amount of energy sold to the grid with trend of renewable generation.

Over time, dissipation loss associated with storage devices increases. In our model the dissipation loss is captured in the system dynamics (3) through factor $\eta_i \ \forall i \in \mathcal{N}$. This factor captures the fraction of stored energy that is retained over one time period, therefore, a value of 1.0 indicates no losses. An increase in dissipation loss (lower η_i value) decreases the effective capacity of storage device and hence, the overall operating costs increase as seen in Figure 5.

V. Conclusion

In this paper, we presented

- *A two-scale MSLP model for distributed storage control:* Our two-scale multistage stochastic linear programming formulation incorporates conventional generation as an offline decision which is decided prior to realization of uncertainty. This decision directly impact all the stages in the adaptive phase. The adaptive phase captures the evolution of distributed storage devices which is optimized along with utilization of power network and operating reserves in response to renewable generation observed at a higher frequency.
- *A scalable sequential sampling algorithm:* The stochastic dynamic linear programming algorithm which was designed to tackle the two-scale formulation with stagewise independent stochastic processes. This algorithm is a dynamic extension of regularized two-stage stochastic decomposition [44], and like its predecessor, does not rely on probability distribution information. The computational results compare our algorithm with SDDP. While SDDP relies on probability distribution information for approximating the cost-to-go function, SDLP overcomes this need and works directly with data sources. This feature makes it amenable to be used with simulators which are often at the disposal of power system operators. The results indicate that SDLP provides results which are not only reliable, but are also statistically indistinguishable from SDDP. Our computational experiments also demonstrated the capability of our algorithm to use scenarios generated from an external simulator. These results provide the first evidence of computational benefits provided by a sequential sampling approach.

Although the computational study presented in this paper was restricted to a single coarse timescale decision, our two-scale framework can accommodate sequential decisions at coarse timescale as well. However, an implementation of such a scheme requires an understanding of termination criteria of adaptive phase optimization. Further, our framework also allows us to create policies in a data-driven manner and is applicable to real scale power systems. We are currently studying these extensions, and results from these experiments will be presented in the future.

Acknowledgment

The authors would like to thank the editor and the referees for their insightful and timely comments.

References

[1] R. Sioshansi, P. Denholm, and T. Jenkin, "Market and policy barriers to deployment of energy storage," *SIAM J. Appl. Math.*, vol. 1, no. 2, pp. 47–63, 2012.
[2] *U.S. Department of Energy Global Energy Storage Database*. Accessed on Aug. 25, 2015. [Online]. Available: http://www.energystorageexchange.org/
[3] "Technology roadmap: Energy storage," Int. Energy Agency, Paris, France, Tech. Rep., Mar. 2014.
[4] F. Graves, T. Jenkin, and D. Murphy, "Opportunities for electricity storage in deregulating markets," *Elect. J.*, vol. 12, no. 8, pp. 46–56, 1999.
[5] R. Walawalkar, J. Apt, and R. Mancini, "Economics of electric energy storage for energy arbitrage and regulation in New York," *Energy Policy*, vol. 35, no. 4, pp. 2558–2568, 2007.
[6] R. Sioshansi, P. Denholm, T. Jenkin, and J. Weiss, "Estimating the value of electricity storage in PJM: Arbitrage and some welfare effects," *Energy Econ.*, vol. 31, no. 2, pp. 269–277, 2009.
[7] R. H. Byrne and C. A. Silva-Monroy, "Estimating the maximum potential revenue for grid connected electricity storage: Arbitrage and regulation," Sandia Nat. Lab., Albuquerque, NM, USA, Tech. Rep. SAND2012-3863, Dec. 2012.
[8] R. Sioshansi, "Increasing the value of wind with energy storage," *Energy J.*, vol. 32, no. 2, pp. 1–30, 2011.
[9] J. B. Greenblatt, S. Succar, D. C. Denkenberger, R. H. Williams, and R. H. Socolow, "Baseload wind energy: Modeling the competition between gas turbines and compressed air energy storage for supplemental generation," *Energy Policy*, vol. 35, no. 3, pp. 1474–1492, 2007.
[10] P. Harsha and M. Dahleh, "Optimal management and sizing of energy storage under dynamic pricing for the efficient integration of renewable energy," *IEEE Trans. Power Syst.*, vol. 30, no. 3, pp. 1164–1181, May 2015.
[11] D. R. Jiang and W. B. Powell, "Optimal hour-ahead bidding in the real-time electricity market with battery storage using approximate dynamic programming," *INFORMS J. Comput.*, vol. 27, no. 3, pp. 525–543, 2015.
[12] X. Xi, R. Sioshansi, and V. Marano, "A stochastic dynamic programming model for co-optimization of distributed energy storage," *Energy Syst.*, vol. 5, no. 3, pp. 475–505, 2014.
[13] J. H. Kim and W. B. Powell, "Optimal energy commitments with storage and intermittent supply," *Oper. Res.*, vol. 59, no. 6, pp. 1347–1360, 2011.

[14] P. Mokrian and M. Stephen, "A stochastic programming framework for the valuation of electricity storage," in *Proc. 26th USAEE/IAEE North Amer. Conf.*, Ann Arbor, MI, USA, 2006, pp. 24–27.
[15] P. D. Brown, J. A. P. Lopes, and M. A. Matos, "Optimization of pumped storage capacity in an isolated power system with large renewable penetration," *IEEE Trans. Power Syst.*, vol. 23, no. 2, pp. 523–531, May 2008.
[16] M. T. Vespucci, F. Maggioni, M. I. Bertocchi, and M. Innorta, "A stochastic model for the daily coordination of pumped storage hydro plants and wind power plants," *Ann. Oper. Res.*, vol. 193, no. 1, pp. 91–105, 2012.
[17] H. Gangammanavar, S. Sen, and V. M. Zavala, "Stochastic optimization of sub-hourly economic dispatch with wind energy," *IEEE Trans. Power Syst.*, vol. 31, no. 2, pp. 949–959, Mar. 2016.
[18] S. Sen, L. Yu, and T. Genc, "A stochastic programming approach to power portfolio optimization," *Oper. Res.*, vol. 54, no. 1, pp. 55–72, 2006.
[19] R. Jiang, J. Wang, and Y. Guan, "Robust unit commitment with wind power and pumped storage hydro," *IEEE Trans. Power Syst.*, vol. 27, no. 2, pp. 800–810, May 2012.
[20] C. Abbey and G. Joos, "A stochastic optimization approach to rating of energy storage systems in wind-diesel isolated grids," *IEEE Trans. Power Syst.*, vol. 24, no. 1, pp. 418–426, Feb. 2009.
[21] Numerical Weather Prediction. *National Oceanic and Atmospheric Administration*. Accessed on Aug. 25, 2015 [Online]. Available: https://www.ncdc.noaa.gov
[22] J. Eyer and G. Corey, "Energy storage for the electricity grid: Benefits and market potential assessment guide," Sandia Nat. Lab., Albuquerque, NM, USA, Tech. Rep. SAND2010-0815, Feb. 2010.
[23] J. M. Morales, R. Mínguez, and A. J. Conejo, "A methodology to generate statistically dependent wind speed scenarios," *Appl. Energy*, vol. 87, no. 3, pp. 843–855, 2010.
[24] M. S. Miranda and R. W. Dunn, "Spatially correlated wind speed modelling for generation adequacy studies in the U.K.," in *Proc. IEEE Power Eng. Soc. Gen. Meeting*, Tampa, FL, USA, 2007, pp. 1–6.
[25] H. Lütkepohl, *New Introduction to Multiple Time Series Analysis*. Heidelberg, Germany: Springer, 2007.
[26] J. Lavaei and S. H. Low, "Convexification of optimal power flow problem," in *Proc. 48th Annu. Allerton Conf. Commun. Control Comput. (Allerton)*, Monticello, IL, USA, Sep. 2010, pp. 223–232.
[27] J. R. Birge and F. Louveaux, *Introduction to Stochastic Programming* (Springer Series in Operations Research and Financial Engineering). New York, NY, USA: Springer, 2011.
[28] J. R. Birge, "Decomposition and partitioning methods for multistage stochastic linear programs," *Oper. Res.*, vol. 33, no. 5, pp. 989–1007, 1985.
[29] J. M. Mulvey and A. Ruszczyński, "A new scenario decomposition method for large-scale stochastic optimization," *Oper. Res.*, vol. 43, no. 3, pp. 477–490, 1995.
[30] R. T. Rockafellar and R. J.-B. Wets, "Scenarios and policy aggregation in optimization under uncertainty," *Math. Oper. Res.*, vol. 16, no. 1, pp. 119–147, Feb. 1991.
[31] J. Dupačová, G. Consigli, and S. W. Wallace, "Scenarios for multistage stochastic programs," *Ann. Oper. Res.*, vol. 100, nos. 1–4, pp. 25–53, 2000.
[32] J. Dupačová, N. Gröwe-Kuska, and W. Römisch, "Scenario reduction in stochastic programming," *Math. Program.*, vol. 95, no. 3, pp. 493–511, 2003.
[33] M. V. F. Pereira and L. M. V. G. Pinto, "Multi-stage stochastic optimization applied to energy planning," *Math. Program.*, vol. 52, nos. 1–3, pp. 359–375, 1991.
[34] A. Gjelsvik, B. Mo, and A. Haugstad, *Long- and Medium-term Operations Planning and Stochastic Modelling in Hydro-dominated Power Systems Based on Stochastic Dual Dynamic Programming*. Heidelberg, Germany: Springer, 2010, pp. 33–55.
[35] G. Infanger and D. P. Morton, "Cut sharing for multistage stochastic linear programs with interstage dependency," *Math. Program.*, vol. 75, no. 2, pp. 241–256, 1996.
[36] A. B. Philpott and Z. Guan, "On the convergence of stochastic dual dynamic programming and related methods," *Oper. Res. Lett.*, vol. 36, no. 4, pp. 450–455, 2008.
[37] A. B. Philpott and V. L. de Matos, "Dynamic sampling algorithms for multi-stage stochastic programs with risk aversion," *Eur. J. Oper. Res.*, vol. 218, no. 2, pp. 470–483, 2012.
[38] S. Sen and Y. Liu, "Mitigating uncertainty via compromise decisions in two-stage stochastic linear programming: Variance reduction," *Oper. Res.*, vol. 64, no. 6, pp. 1422–1437, 2016.
[39] S. Sen and Z. Zhou, "Multistage stochastic decomposition: A bridge between stochastic programming and approximate dynamic programming," *SIAM J. Optim.*, vol. 24, no. 1, pp. 127–153, 2014.
[40] S. Sen, "Stochastic programming," in *Encyclopedia of Operations Research and Management Science*, S. I. Gass and M. C. Fu, Eds. New York, NY, USA: Springer, 2013, pp. 1486–1497.
[41] Y. M. Ermoliev, "Stochastic quasigradient methods and their application to system optimization," *Stochastics*, vol. 9, nos. 1–2, pp. 1–36, 1983.
[42] A. Nemirovski, A. Juditsky, G. Lan, and A. Shapiro, "Robust stochastic approximation approach to stochastic programming," *SIAM J. Optim.*, vol. 19, no. 4, pp. 1574–1609, 2009.
[43] A. Ruszczyński, "A regularized decomposition method for minimizing a sum of polyhedral functions," *Math. Program.*, vol. 35, no. 3, pp. 309–333, 1986.
[44] J. L. Higle and S. Sen, "Finite master programs in regularized stochastic decomposition," *Math. Program.*, vol. 67, nos. 1–3, pp. 143–168, 1994.
[45] R. D. Christie. (Aug. 1999). *Power Systems Test Case Archive*. Accessed on Aug. 1, 2015. [Online]. Available: http://www.ee.washington.edu/research/pstca/
[46] A. Shapiro, "Analysis of stochastic dual dynamic programming method," *Eur. J. Oper. Res.*, vol. 209, no. 1, pp. 63–72, 2011.
[47] W. G. Manuel, "Energy storage study 2014," Turlock Irrigation District, Turlock, CA, USA, accessed on Feb. 15, 2014. [Online]. Available: http://www.energy.ca.gov/assessments/ab2514_reports/Turlock_Irrigation_District/
[48] C. W. Potter *et al.*, "Creating the dataset for the western wind and solar integration study (U.S.A.)," *Wind Eng.*, vol. 32, no. 4, pp. 325–338, 2008.

Harsha Gangammanavar received the M.S. degree in electrical engineering and the Ph.D. degree in operations research from Ohio State University in 2009 and 2013, respectively. He is an Assistant Professor with the Department of Engineering Management, Information, and Systems, Southern Methodist University. He has held the position of a Post-Doctoral Fellow with Industrial Engineering, Clemson University, and a Visiting Assistant Professor with the Daniel J. Epstein Department of Industrial and Systems Engineering, University of Southern California. His research interests are focused on stochastic optimization, and its application in power systems planning and operations.

Suvrajeet Sen is a Professor with the Daniel J. Epstein Department of Industrial and Systems Engineering, University of Southern California. He has held several other positions, including a Professor with the University of Arizona, and a Program Director of Operations Research, as well as Service Enterprise Systems at the National Science Foundation. He has led a group of world-renowned OR visionaries to identifying new themes of OR for problems motivated by Grand Challenges of the National Academy of Engineering. His research is devoted to many categories of optimization models, algorithms, and applications of stochastic programming problems. He was a recipient of the 2015 INFORMS Computing Society Prize for their work on stochastic mixed-integer programming. He is a fellow of INFORMS.